

Effects of the Annealing and Exposure on the Optical and Photoinduced Properties of Amorphous $(As_4S_3Se_3)_{1-x}:Sn_x$ Thin Films

O.V. IASENIUC

*Institute of Applied Physics, Academy of Sciences of Moldova
5 Academiei str., MD-2028 Chisinau, Republic of Moldova
oxygena08@rambler.ru*

Abstract – The influence of the heat treatment and light exposure on optical and photoinduced properties of $(As_4S_3Se_3)_{1-x}:Sn_x$ thin films are investigated. The thin films were characterized by X-Ray diffraction (XRD), and optical absorption spectroscopy. The XRD measurements showed that the Sn impurities in the $(As_4S_3Se_3)_{1-x}:Sn_x$ essentially don't change the shape of the FSDP of the X-ray diffraction patterns, the intensity and the position of the first sharp diffraction peak non-monotonously depend on the Sn concentration. By the optical absorption spectroscopy the transmission spectra of bulk materials and thin films of $(As_4S_3Se_3)_{1-x}:Sn_x$ ($x=0-10$ at.%) in the visible and near infrared regions have been studied. The modifications of optical parameters (optical band gap E_g^{opt} , absorption coefficient α , refractive index n) under light irradiation by halogen lamp of the amorphous thin films with different amount of Sn were measured and calculated. On the transmission spectra the red shift of the fundamental absorption edge under light exposure was observed, and the values of the optical band gap E_g^{opt} from the graphics in Tauc coordinates ($\alpha h\nu/2=A(h\nu - E_g)$) were obtained. The dispersion of the refractive index was examined. Moreover, manifestation of partial reversibility of the optical absorption after annealing was demonstrated. The relaxation of the relative optical transmission $T/T_0=f(t)$ under the light exposure ($\lambda=633$ nm) for amorphous $(As_4S_3Se_3)_{1-x}:Sn_x$ thin films also was investigated. The relaxation curves of photodarkening under light irradiation were processing using the stretched exponential presentation of the data: $T(t)/T(0) = A_0 + A \exp[-(t-t_0)/\tau]^{(1-\beta)}$. Where t – is the exposure time, τ – is the apparent time constant, A – characterizes the exponent amplitude, t_0 – and A_0 – are the initial coordinates, and β - is the dispersion parameter ($0 < \beta < 1$), and were estimated by a computer program.

Index Terms – Chalcogenide glasses, amorphous films, refractive index, annealing, photodarkening effect.

I. INTRODUCTION

Chalcogenide vitreous semiconductors (ChVS) of the As-S-Se system exhibit photostructural transformations with reversible and irreversible properties, and are promising materials as registration media for holography and optical information, for fabrication of diffractive elements, and other optoelectronic applications [1-3]. As shown in [4], the illumination of the amorphous thin films of ChVS with light with photon energy close or even lower, after absorption leads to the creation of the electron-hole pairs. Their subsequent recombination brings bond reforming processes, that is microscopic network change, brings structural, mechanical, optical, etc. changes in these materials. The optical changes involve photo increases refractive index n and absorption edge shift $\Delta\alpha$ to the longer wavelength region. For amorphous As-S-Se thin films, it was found, that photo-irradiation causes increase refractive index value in the completely considered region (0.4-2.5 nm) [4].

It is well known that the optical properties which are characterized by optical parameters – absorption coefficient α , refractive index n , optical band gap E_g^{opt} depend on the glass composition. In the last years, a special attention has

been devoted to the influence on the photostructural transformation in amorphous thin films doped with metal impurity [5-8]. It was shown, that the Sn impurity introduced in the As_2Se_3 , $AsSe$, and Sb_2Se_3 glass network reduces the photodarkening effect. According to Mössbauer spectroscopy of ^{119}Sn in the $As_2Se_3:Sn$ glassy system, new tetrahedral $Sn(Se_{1/2})_4$ and quasi-octahedral $SnSe$ structural units can be formed, and which influence the degree of photostructural transformations [6]. The advantages of application of amorphous thin films of ChVS as gas sensors and for registration of optical information were shown in [9-11]. Some optical properties of $(As_2S_{1.5}Se_{1.5})_{0.99}:Sn_{0.01}$ were reported in [12].

The present paper deals with the optical transmission spectra and the modifications of optical parameters (optical band gap E_g , absorption coefficient α , refractive index n) under light irradiation and heat treatment of amorphous $(As_4S_3Se_3)_{1-x}:Sn_x$ thin films with different amounts of Sn. The relaxation of photodarkening effect under light exposure with different wavelength ($\lambda = 633$ nm) also was investigated.

II. EXPERIMENTAL

The bulk chalcogenide glasses As_2S_3 , As_2Se_3 , $(\text{As}_2\text{S}_3)_{0.5}:(\text{As}_2\text{Se}_3)_{0.5}$, and $[(\text{As}_2\text{S}_3)_{0.5}:(\text{As}_2\text{Se}_3)_{0.5}]_{1-x}:\text{Sn}_x$ ($0 \leq x \leq 10$ at.%) (or $(\text{As}_4\text{S}_3\text{Se}_3)_{1-x}:\text{Sn}_x$) were prepared from the starting elements of 6N (As, S, Se, Sn) purity by a conventional melt quenching method. The starting components elements $\text{As}_4\text{S}_3\text{Se}_3$ and Sn were mixed in quartz ampoules and then evacuated to pressure of $P \sim 10^{-5}$ torr, sealed and heated to temperature $T=900$ °C at the rate of 1 °C/min. The quartz tubes were held at this temperature for 48 hours for the homogenization and then slowly quenched in the heating furnace. X-Ray Diffraction (XRD) of samples was recorded at room temperature using DRON-UM1 diffractometer with $\text{Fe-K}\alpha$ radiation ($\lambda=1.93604$ Å), with Mn filter by $\theta/2\theta$ scanning method.

For the optical measurements of bulk samples were prepared the plan parallel plates of thickness about $d = 2-4$ mm, and polished. The thin-film samples with a thickness of $d = 1.5 \pm 0.02$ μm were prepared by flash thermal evaporation method in vacuum of the synthesized initial glasses onto glass substrates held at $T_{\text{subs}} = 100$ °C. For optical transmission spectra measurements, a UV/VIS ($\lambda = 300-800$ nm), the 61 NIR ($\lambda = 800-3500$ nm) Specord's CARLZEISS Jena production and Spectrum 100 FTIR Spectrometer (PerkinElmer) ($\lambda = 1280-25000$ nm) were used. For calculation of the optical constants from the transmission spectra, we used the method proposed by Swanepoel and Tauc [13, 14] and the computer program PARAV-V1.0 (www.chalcogenide.eu.org) [15]. For study of red shift edge of transmission spectra of thin films the halogen lamp ($\lambda = 400-700$ nm, with infrared filter, with a light density $2 \times 10^4 \text{Lx}$) was used as a source of light exposure. To initiate photostructural transformations in thin film samples, continuous He-Ne lasers ($\lambda = 633$ nm, $P = 0.6$ mW and $\lambda = 540$ nm, $P = 0.75$ mW) were used as a source of light exposure. The relaxation of the transmission curves was measured both at $\lambda=630$ nm and $\lambda=540$ nm wavelengths during the excitation. The laser spot on the sample was about 1 mm in diameter. For data acquisition the experimental set-up included a digital build-in PC-card PCI-1713A connected with the registration module.

III. RESULTS AND DISCUSSION

A) X-Ray diffraction patterns.

Using the X-Ray Diffraction method were obtained the diffraction patterns in the range of diffraction angles 2θ from 10° to 80° (θ is the Bragg angle) for the chalcogenide glasses As_2S_3 , As_2Se_3 , $\text{As}_4\text{S}_3\text{Se}_3$, and $\text{As}_4\text{S}_3\text{Se}_3:\text{Sn}_x$ ($x = 0.01, 0.02, 0.04, 0.06, 0.07$ и 0.10). Fig. 1 indicates the angular distribution of X-Ray diffraction intensity for As_2S_3 , As_2Se_3 , and $\text{As}_4\text{S}_3\text{Se}_3$ prepared glasses. The position of the First Sharp Diffraction Peak (FSDP) for As_2S_3 is $2\theta=22.47^\circ$ and increase up to $2\theta=24.60^\circ$ for As_2Se_3 . For the intermediate composition $\text{As}_4\text{S}_3\text{Se}_3$ the maximum of the FSDP is situated at $2\theta=23.00^\circ$ (Fig.1). These spectra represent a sum of diffraction patterns of izostructural vitreous As_2S_3

and As_2Se_3 with three broad lines of diffractograms and which are similar to the envelope of the rounded lines of the spectra of crystalline As_2S_3 and As_2Se_3 . It can be assume about the microcrystalline state of the investigated glasses – existence of domains with ordered structure with dimensions about 15 – 20 Å. Previously a analogy between the structure of vitreous and crystalline states of As_2S_3 was vindicated by short-range order investigations – interatomic distances and coordination numbers – with the add of the radial distribution function [16]. The careful investigations of the FSDP of vitreous As_2S_3 and As_2Se_3 show that they have a similar structure [17]. According to [17], the first coordination spheres (first order neighbour position) of a central atom in the structure is $r_1=2.414$ Å for As_2Se_3 , and $r_1=2.306$ Å for As_2S_3 , respectively. The second coordination spheres (second order neighbour position) of a central atom in the structure is $r_2=3.625$ Å for As_2Se_3 , and $r_2=3.475$ Å for As_2S_3 , respectively.

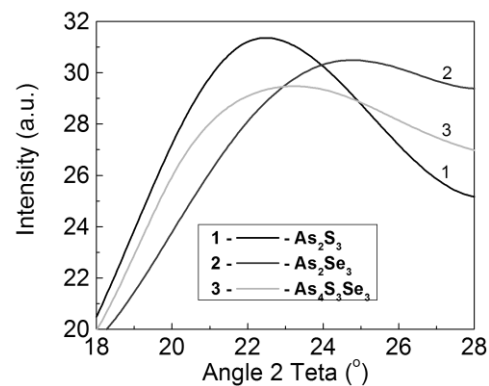


Fig.1. First sharp diffraction peak (FSDP) in the X-ray diffraction patterns of As_2S_3 (1), As_2Se_3 (2), and $\text{As}_4\text{S}_3\text{Se}_3$ (3).

It was established that between As_2S_3 and As_2Se_3 layers act Van der Waals forces with a reduced covalent component. The interaction forces between layers are hundred times weaker than the binding forces between the layers. According the [17], the structure of the glasses represent as an interlinking of As-S₃ and As-Se₃ pyramids that forms rings with 6 units. The arsenic atoms are situated at the top of the pyramid, while the chalcogen atoms form the basis.

As was shown, the crystalline semiconductors are characterized by long-range order (LRO), i.e. there is a good correlation between the position in the network, of the each two atoms, that can't be said about the non-crystalline semiconductors [18, 19]. For non-crystalline semiconductors, there is only short-range order (SRO), which belongs to the individual atoms in the first coordination sphere. As in chalcogenide glasses range order can be extended to several interatomic distances, the new concept of the average order was introduced (MRO).

The Sn concentration in the mixed glasses $\text{As}_4\text{S}_3\text{Se}_3:\text{Sn}_x$ essentially don't change the shape of the FSDP of the X-ray diffraction patterns (Fig.2). In general, the diffraction patterns of the $\text{As}_4\text{S}_3\text{Se}_3:\text{Sn}_x$ glasses are similar and form three wide lines, the maxima of which correspond to the interlayer distances $d \sim 4.8 - 2.8 - 1.7$ Å. As in the case of $\text{As}_2\text{Se}_3:\text{Sn}_x$ [20], the angular position of

the FSDP in the $As_4S_3Se_3:Sn_x$ slightly depend on the Sn concentration.

Fig.3 shows the dependences of the peaks intensities vs. concentrations of tin of the three diffraction peaks of chalcogenide glass $As_4S_3Se_3:Sn_x$ situated at $2\theta \sim 22 \div 24^\circ$, $2\theta \sim 40 \div 42^\circ$, and $2\theta \sim 62 \div 70^\circ$, respectively.

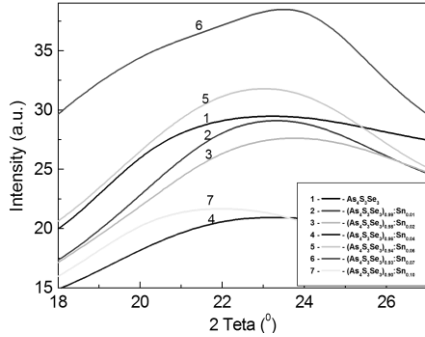


Fig.2. First sharp diffraction peak (FSDP) in the X-ray diffraction patterns of $As_4S_3Se_3$ (1), $(As_4S_3Se_3)_{0.99}:Sn_{0.01}$ (2), $(As_4S_3Se_3)_{0.98}:Sn_{0.02}$ (3), $(As_4S_3Se_3)_{0.96}:Sn_{0.04}$ (4), $(As_4S_3Se_3)_{0.94}:Sn_{0.06}$ (5), $(As_4S_3Se_3)_{0.93}:Sn_{0.07}$ (6), $(As_4S_3Se_3)_{0.90}:Sn_{0.1}$ (7).

The intensity of the FSDP shows a non-linear behavior with the different amount of doping of Sn. The maximum intensity is reached around 6 at.% Sn in $As_4S_3Se_3:Sn_x$, while in the case of $As_2S_3:Sn_x$ the maximum intensity is situated at the tin concentration at ~ 2 at.% Sn. The similar behavior was found for the 2-nd and the 3-rd diffraction peaks.

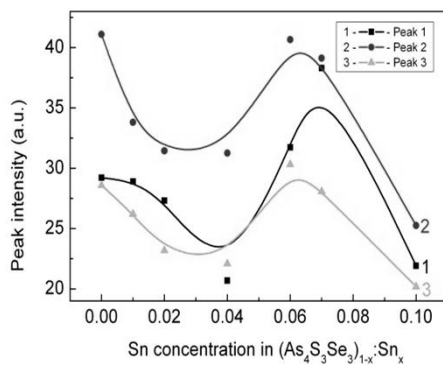


Fig.3. Dependence of the angular position of the diffraction peaks vs. concentration of tin in the chalcogenide glass $As_4S_3Se_3:Sn_x$.

According to [20], when Sn is added in ChGS like As_2Se_3 or As_2S_3 , due to the tetrahedral disposal of the sp^3 bonds in the chalcogen the dopant atom inserted in the network increases the thickness of the layered configuration as revealed by the significant shift of the FSDP towards lower angles. This insertion corresponds to the introduction in the glass network of the structural units of the type $SnSe_2$ or SnS_2 , and the same fact was confirmed by the Mössbauer spectroscopy experiments [6].

B) The transmission spectra

The mid-IR transmission spectra of some $[(As_2S_3)_{0.5}:(As_2Se_3)_{0.5}]_{1-x}:Sn_x$ bulk glasses and UV-VIS spectra for as-deposited films were reported in [21]. It

was shown, that the characteristic absorption bands for pure As_2S_3 at $\nu = 5190, 3617, 3522, 1857,$ and 1597 cm^{-1} are significantly reduced upon doping with Sn.

The visible transmission spectra of the amorphous $(As_4S_3Se_3)_{1-x}:Sn_x$ thin films after excitation of light and heat treatment are presented in fig.4. As in the case of as-deposited thin films, increasing of Sn concentration in amorphous $(As_4S_3Se_3)_{1-x}:Sn_x$ thin films leads to shift the absorption edge in the red region of the spectra.

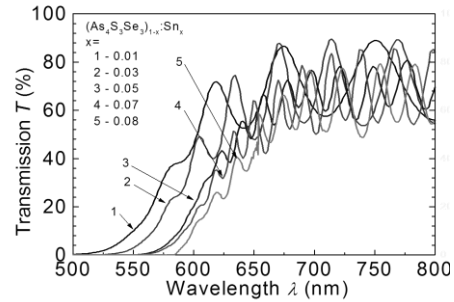


Fig.4. The transmission spectra of amorphous $[(As_4S_3Se_3)_{1-x}:Sn_x]$ thin films, x: 1-1%; 2-3%; 3-5%; 4-7%, 5-8%.

From spectra (Fig.4) $T = f(\lambda)$, using the expressions:

$$\alpha = \frac{1}{d} \ln \frac{(1-R)^2}{T}, n = \left[M + (M^2 - n_s^2)^{1/2} \right]^{1/2}, \quad (1)$$

where $M = \frac{2n_s}{T_m} - \frac{n_s^2 + 1}{2}$ and the dependence $(\alpha h\nu)^{1/2} =$

$A(h\nu - E_g)$, we calculated the absorption coefficient α , the refractive index n , and the value of the optical band gap E_g , respectively. Here d is the thickness of the sample (measured with a Linnik interferometer), R is the reflection, n_s is the refractive index of glass substrate, T_m is the experimental values of transmission minimum points of particular fringes of transmission spectra, and A is a constant.

In chalcogenide glasses, the absorption edge is broader than in crystalline analogues, and this is caused by a broad energy distribution of electronic states in the band gap due to disorder and defects. The absorption edge in the high absorption region ($\alpha > 10^4 \text{ cm}^{-1}$) is described by the quadratic function

$$\alpha \propto \frac{1}{h\nu} (h\nu - E_g)^2, \quad (2)$$

and when plotted in the Tauc co-ordinates $(\alpha h\nu)^{1/2}$ vs. $(h\nu)$ [22] gives the value of the optical band gap E_g determined as the energy difference between the onsets of exponential tails of the allowed conduction bands [23].

Fig.5 represents the transmission spectra of the amorphous $[(As_4S_3Se_3)_{0.03}:Sn_{0.97}]$ thin film for as deposited and after light exposure. As can be seen, in the transmission spectra, the light exposure sifts of the absorption edge in the red region of the spectrum, e.g. the photodarkening effect take place, and the degree of modification of the absorption edge depends on the Sn concentration.

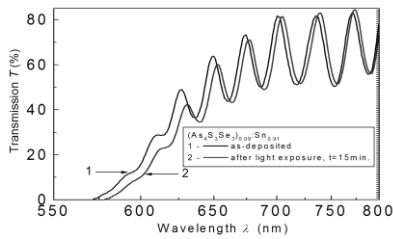


Fig.5. Transmission spectra of the amorphous $[(As_4S_3Se_3)_{0.03}:Sn_{0.97}]$ thin film as 1-deposited, 2-after light exposure.

Fig.6 represents the transmission spectra of amorphous $(As_4S_3Se_3)_{0.97}:Sn_{0.03}$ thin film for the as-deposited samples, after light exposure and after light exposure and annealed at $T_{ann}=100\text{ }^\circ\text{C}$ during 30 min. The light exposure sifts the absorption edge in the red region of the spectrum, while the heat treatment partially returns to its original position. This is well-known reversible photodarkening effect.

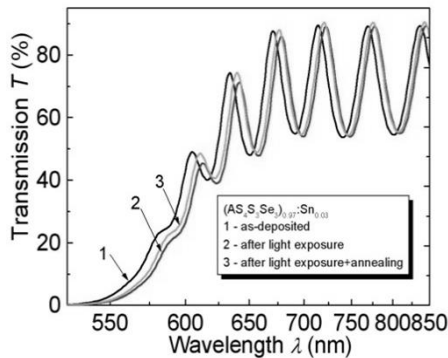


Fig.6. Transmission spectra of the amorphous $(As_4S_3Se_3)_{0.97}:Sn_{0.03}$ thin film 1-as-deposited, 2-after light exposure, 3-after annealing,.

The Sn impurities in amorphous $(As_4S_3Se_3)_{1-x}:Sn_x$ thin film increase the absorption coefficient α and decrease the optical band gap E_g^{opt} , as was observed in the case of the amorphous AsSe:Sn films [18]. These peculiarities indicate that the tin impurities in chalcogenide glasses induce a broadening of the electronic tail states in the conduction bands and shift the Uriah edge in the red region of the spectrum. This broadening of the electronic tail states can be attributed to the formation of new tetrahedral structural units containing Sn [5], which leads to an additional structural disorder to that existing in the matrix of chalcogenide glass. Figure 7 represents the transmission spectra of the amorphous $(As_4S_3Se_3)_{0.97}:Sn_{0.03}$ thin film for as deposited, after light exposure and after heart treatment. It is evident that illumination of the samples with the actinic light causes a red shift of the absorption edge thereby decreasing the optical band gap.

C) The photodarkening relaxation

The relaxation of the relative optical transmission $T/T_0 = f(t)$ under light exposure at $\lambda = 633\text{ nm}$ for amorphous $(As_4S_3Se_3)_{1-x}:Sn_x$ thin films is shown in Fig.8. At a constant light intensity, the presented dependences

characterize the decay of the film optical transmittance with the increase in the dose of absorbed photons.

To obtain a unified basis for comparison of the transmission relaxation $T(t)/T(0)$ curves, we used the so-called stretched exponential presentation for the relaxation curves in the form

$$T(t)/T(0) = A_0 + A \exp[-(t-t_0)/\tau]^{(1-\beta)}, \quad (3)$$

here t is the exposure time, τ is the apparent time constant, A characterizes the exponent amplitude, t_0 and A_0 are the initial coordinates, and α is the dispersion parameter ($0 < \beta < 1$).

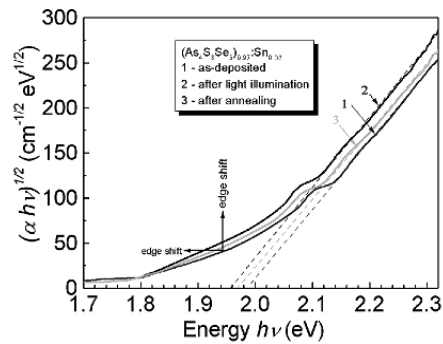


Fig. 7. Absorption spectra in the Tauc coordinates $(\alpha h\nu)^{1/2} = A(h\nu - E_g)$ of the $(As_4S_3Se_3)_{0.97}:Sn_{0.03}$ thin film: 1-as deposited, 2-after light exposure, 3-after light exposure and heat treatment.

Fig.9 represents the dependence of parameters τ and β vs. Sn concentration in amorphous $(As_3S_4Se_4)_{1-x}:Sn_x$ thin films at excitation with $\lambda = 633\text{ nm}$.

For the obtained relaxation curves, a rather wide scatter of parameters is observed for samples of the different composition. For doped samples, this dispersion may be caused by the fact that the concentration and distribution uniformity of the impurity is not adequately preserved along the film at deposition. But the relaxation curves are significantly different in the case of non-doped $(As_2S_3)_{0.5}:(As_2Se_3)_{0.5}$. The main cause is the difference in thickness. For these samples, the effect of interference of light reflected at the front and rear film boundaries significantly changes the amount of absorbed light leading to a strong dependence of photodarkening at a fixed laser wavelength on film thickness [6].

The photodarkening phenomenon in chalcogenide glass films under illumination has no plain explanation up to now in spite of detailed investigation and a series of models advanced for interpretation of it. The red shift of the absorption edge, which indicates the narrowing of the optical gap of the film at photodarkening, is believed to be due to the broadening of the valence band, the top of which is formed mainly by states of lone-pare electrons of the chalcogen atom. Several models have been put forward to substantiate this broadening with a particular individual atom regarded as an initial object of photoexcitation [24, 25]. Recently, a novel model for photodarkening in $a-As_2Se(S)_3$ has been proposed [21, 26], in which photoexcited charge carriers in extended states are considered to be responsible for photodarkening.

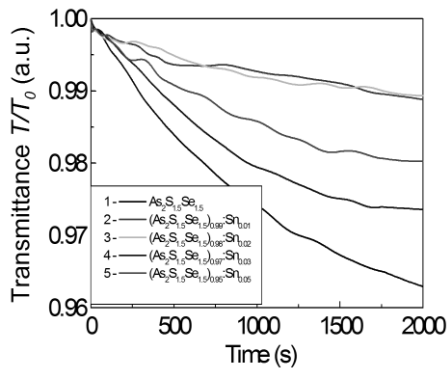


Fig.8. The relaxation curves of photodarkening $T/T_0=f(t)$ for amorphous $(As_3S_4Se_4)_{1-x}:Sn_x$ thin films. Excitation with He-Ne laser $\lambda = 633$ nm.

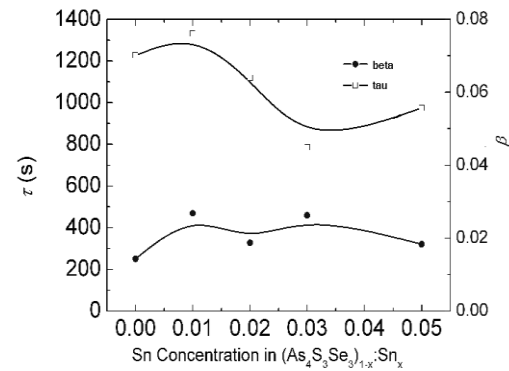


Fig.9. Dependencies of parameters τ and β vs. Sn concentration in amorphous $(As_3S_4Se_4)_{1-x}:Sn_x$ thin films at excitation with $\lambda = 633$ nm.

Unlike the previous conceptions, the new model takes into account the layered cluster structure of a chalcogenide glass. During exposure, the layer is negatively charged due to the capture of photoexcited electrons, and repulsive forces are built between the layers. These forces cause an enlargement in the interlayer distance (leading to photoexpansion) and slip motion along the layers. The last mentioned process alters the interaction of lone-pair electrons between the layers leading to a photodarkening effect.

In the absence of tin, the arsenic chalcogenide glass is formed of corrugated and disordered layer domains with some correlation between them. This correlation leads to a rather compact packing with low inter-configurational distance. Upon the introduction of Sn, due to the tetrahedral disposal of the sp^3 bonds with the chalcogens, the dopant atom inserted in the network increases the thickness of the layered configuration as revealed by the significant shift of the FSDP towards lower angles. This insertion corresponds, in fact, to the introduction of the structural units of the type $SnSe_2$ in the network. The effect is greater for higher dopant content but only up to a certain concentration, because further the separation of the reciprocally ordered configurations is interrupted by increasing interconnection between layers followed by the transition to three-dimensionally (3D) connected network. The transition is preceded by the appearance of structural units of the Sn-Se type. Then, the direct consequence of this transition will be shown in the intensity of the FSDP, which gradually disappears. The interruption of the two-dimensional structure and transition is probably due to a more ionic nature of the Sn-Se bonds.

The tin impurity strongly affects on the network of the host glass inducing changes in both short-range and medium-range order; in particular, they have a significant effect on the structural layers and the pattern of their relative motion. This fact clearly indicates a strong retardation of the slip motion of the structure layers due to the presence of impurity. Since tin tends to form directional bonds when introduced in the host glass, and especially during the annealing process, some bridging bonds should appear between the layers.

The structure of the glasses that contains a tin impurity requires, therefore, some excess slip forces, i.e., leads to greater exposition dose and time constants. Furthermore, the formation of clusters, such as of the $SnSe_2$ type, can decrease the density of lone-pair defects typical for AsSe and AsS (i.e., D-centers) thus lowering the charge state of the layers and, finally, the photodarkening.

IV. SUMMARY

The doping of $(As_4S_3Se_3)$ glasses with tin impurities leads to the shift of the absorption edge in the red region of the spectrum and to decreasing of the optical band gap. Under the light exposure the amorphous $(As_4S_3Se_3)_{1-x}:Sn_x$ become darkened, while the heat treatment partially reversed it to the initial position. The relaxation of photodarkening effect in amorphous $(As_4S_3Se_3)_{1-x}:Sn_x$ thin films is described by the stretch exponential function $T(t)/T(0) = A_0 + A \exp[-(t-t_0)/\tau^{(1-\beta)}$. The main feature of the photodarkening effect in the samples under study is that the tin impurities suppressed the photodarkening.

ACKNOWLEDGMENTS

The work is supported by the National Institutional Project no. 11.817.05.03A. The author is kindly grateful to Drs. V.E. Tazlavan and E.P. Colomeico for sample preparation; to Drs. I.A. Cojocar, D.F. Felix, and A.Yu. Meshalkin for some optical measurements; Dr. G.F. Volodina for X-ray diffractions measurements, and Prof. M.S. Iovu for valuable discussion, critical reading of this paper, and his interest in this work.

REFERENCES

- [1] A. Stronski, M. Vlcek, S. Kostyukovich, V. Tomchuk, E. Kostyukovich, S. Svechnikov, A. Kudreavtsev, N.L. Moskalenko, A. Koptyukh, *Study of non-reversible photostructural transformations in $As_{40}S_{60-x}Se_x$ layers applied for fabrication of holographic protective elements*, Sem. Physics, Quantum Electronics & Optoelectronics, 5(3), pp. 284-287, 2002.

- [2] A. Gerbreeders, J. Teteris, *Recording of surface-relief gratings on amorphous As-S-Se films*, J. of Optoelect. and Advanced Materials, 9(10), pp. 3164-3166, (2007).
- [3] M. Reinfelde, J. Teteris, *Surface relief and polarization holographic formation in amorphous As-S-Se films*, J. of Optoelect. and Adv. Mat., 13(11-12), pp. 1531-1533, 2011.
- [4] A. Stronski, M. Vlcek, *Photosensitive properties of chalcogenide vitreous semiconductors in diffractive and holographic technologies, applications*, J. of Optoelectronics and Advanced Materials, 4(3), pp. 699 – 704, 2002.
- [5] M. Iovu, S. Shutov, M. Popescu, *Relaxation of photodarkening in amorphous As-Se films doped with metals*, J. of Non-Cryst.Sol., 299-309, pp. 924-928, 2002.
- [6] P. Boolchand, D. Georgiev, M. Iovu, *Molecular structure and quenching of photodarkening in As₂Se₃:Sn amorphous films*, Chalcogenide Letters, 2(4), pp. 27-34, 2005.
- [7] M. Iovu, P. Boolchand, D. Georgiev, *Photodarkening relaxation in amorphous As₂Se₃ films doped with rare-earth ions*, J. of Optoelectronics and Advanced Materials, 7(2), pp. 763-770, 2005.
- [8] M. Iovu, D. Harea, E. Colomeico, *Some optical properties of thermally deposited Sb₂Se₃:Sn thin films*, Journal of Optoelectronics and Advanced Materials, 10(4), pp. 862-866, 2008.
- [9] D. Tsiulyanu, S. Marian, H - D. Liess, I. Eisele, *Chalcogenide based gas sensors*, J. of Optoelectronics and Advanced Materials, 5(5), pp. 1349 - 1354, 2003.
- [10] S. Marian, D. Tsiulyanu, T. Marian, H. Liess, *Chalcogenide-based chemical sensors for atmospheric pollution control*, Pure Appl. Chem., 73(12), pp. 2001–2004, 2001.
- [11] V. Miniko, I. Indutnyy, P. Shepeliavyy, P. Litvin, *Application of amorphous chalcogenide films for recording of high-frequency phase-relief diffraction gratings*, J. of Optoelectronics and Advanced Materials, 7(3), pp. 1429 – 1432, 2005.
- [12] O. Iaseniuc, A. Andriesh, A. Abashkin, *Optical properties of amorphous (As₂S_{1.5}Se_{1.5})_{0.99}:Sn_{0.01}*, Moldavian J. of the Physical Sciences, 9(3-4), pp. 349-355, 2010.
- [13] J. Tauc, *The optical properties of solids*, North-Holland, Amsterdam, 1970.
- [14] R. Swanepoel, *Determination of the thickness and optical constants of amorphous silicon*, J.Phys.E: Sci.Instrum., 16(12), pp. 1214-1222, 1983.
- [15] A. Ganjoo, R. Golovchak, *Computer program PARAV for calculating optical constants of thin films and bulk materials: Case study of amorphous semiconductors*, J.of Optoelectronics and Advanced Materials, 10(6), pp. 1328-1332, 2008.
- [16] L. Tatariniva, *The structure of amorphous solids and liquids*. M., «SCIENCE», p.151, 1983.
- [17] M. Popescu, A. Andrieș, V. Ciumaș, M. Iovu, S. Șutov, D. Țiuleanu, *Physics of chalcogenide glasses*. Science Bucuresti, Science Chisinau, 1996.
- [18] M. Popescu, *Medium range orders in chalcogenide glasses*, In: Physics and Applications of Non-Crystalline Semiconductors in Optoelectronics, Eds. A.Andriesh & M.Bertolotti, Vol. 36, pp. 215-232 1996.
- [19] M. Popescu, F. Tudorica, A. Andriesh, M. Iovu, S. Shutov, M. Bulgaru, E. Colomeycu, et.al., *Structure and electrophysical properties of tin doped arsenic selenide glasses*, Physics and Engin., No. 3, pp. 3-13, 1995.
- [20] M. Iovu, S. Shutov, A. Andriesh, E. Kamitsos, C. Varsamis, D. Furniss, A. Seddon, M. Popescu, *Spectroscopic studies of bulk As₂S₃ glasses and amorphous films doped with Dy, Sm and Mn*, J. of Optoelectronics and Advanced Materials 3(2), pp. 443-454, 2001.
- [21] D. Wood, J. Tauc, *Weak absorption tails in amorphous semiconductors*, Phys. Review, 5(8), pp. 3144-3151, 1972.
- [22] V. Chacorn, D. Haneman, *Thickness and doping dependence of the optical gap in amorphous hydrogenated silicon films*, Solid State Communications, Elsevier, 65 (7), pp. 609-611, 1988.
- [23] M. Iovu, N. Syrbu, S. Shutov, I. Vasiliev, S. Rebeja, E. Colomeico, M. Popescu, and F. Sava, *Spectroscopical Study of Amorphous AsSe : Sn Films*, Phys. Stat. Solidi A, 175(2), pp. 615-622, 1999.
- [24] G. Pfeiffer, M. Paesler, S. Agarxal, *Reversible photodarkening in amorphous arsenic chalcogenides structural*, J. of Non-Crystalline Solids, 130(2), pp. 111-143, 1991.
- [25] K. Shimakawa, A. Kolobov, S. Elliot, *Photoinduced effects and metastability in amorphous semiconductors and insulators*, Advances in Physics, 44(6), pp. 675-788, 1995.
- [26] K. Shimakawa, N. Yoshida, A.Ganjoo, Y. Kuzukawa, J. Singh, *A model for photostructural changes in amorphous chalcogenides*, Phil.Mag.Lett., 77(3), pp. 153-158, 1998.
- [27] A. Ganjoo, N. Yoshida, and K. Shimakawa, *Photoinduced changes on the structural and electronic properties of amorphous semiconductors*, Recent Research Developments in Applied Physics, 2, pp. 129-150, 1999.
- [28] M. Popescu, *Computer-assisted modeling of photostructural transformations in amorphous As₃Se₂*, J.of Non-Crystalline Solids, 90(1-3), pp. 533-536, 1987.
- [29] D. Gisom, M. Gingerich, E. Frieble, *Radiation-induced defects in glasses: Origin of power-law dependence of concentration dose*, Phys.Rev.Lett., 71(1), pp. 1019-1022, 1993.
- [30] G .Pfister, H. Sher, *Dispersive (non-Gaussian) transient transport in disordered solids*, Advances in Physics, 27, pp. 747-798, 1978.